

University of Dundee

A variable impedance actuator using shape memory alloy

Manfredi, Luigi; Velsink, Florian; Khan, Muhammad Amir Hamza; Cuschieri, Alfred

Published in:
Proceedings Actuator 2016

Publication date:
2016

Document Version
Peer reviewed version

[Link to publication in Discovery Research Portal](#)

Citation for published version (APA):

Manfredi, L., Velsink, F., Khan, M. A. H., & Cuschieri, A. (2016). A variable impedance actuator using shape memory alloy. In H. Borgmann (Ed.), *Proceedings Actuator 2016* (pp. 167-170). [B 1.2] Messe Bremen-HVG Hanseatische Veransaltungs-GMBH.

General rights

Copyright and moral rights for the publications made accessible in Discovery Research Portal are retained by the authors and/or other copyright owners and it is a condition of accessing publications that users recognise and abide by the legal requirements associated with these rights.

- Users may download and print one copy of any publication from Discovery Research Portal for the purpose of private study or research.
- You may not further distribute the material or use it for any profit-making activity or commercial gain.
- You may freely distribute the URL identifying the publication in the public portal.

Take down policy

If you believe that this document breaches copyright please contact us providing details, and we will remove access to the work immediately and investigate your claim.

A variable impedance actuator based on shape memory alloy

L Manfredi, F. L. Velsink, H. Khan, A. Cuschieri

Institute for Medical Science and Technology (IMSaT), University of Dundee, Dundee, UK

Abstract:

Surgical robotic design is challenging mostly because of the restricted working space of the platform necessitating miniaturized actuators and sensors. Compliance is a fundamental requirement of an actuator design for safe atraumatic clinical interaction of the robot with organs and tissues [1]. In the present paper, the authors describe a variable impedance miniaturised rotary actuator (VIMRA) using shape memory alloy (SMA) wires in antagonist configuration, to achieve a high force to weight ratio. The two SMA wires are connected to a pulley providing two forces, which can be independently controlled to adjust the joint stiffness.

Keywords: Smart materials, variable stiffness actuator, robotic

Introduction

Several designs have been proposed for surgical robots [2]-[3]. Most however, employ cable transmission with location of the actuators outside of the robot [7]-[9]. The advantage of this approach is to reduce the size of the robot, keeping both weight and inertia low. The disadvantage of this design is that the number of cables needed increases with the number of joints, which limits the degree of freedoms (DoFs) of the robot. An alternative design solution consists of using actuators embedded in the body of the robot, but this requires use of small and light actuators. Shape memory alloys (SMAs) are materials that can provide a solution to this miniaturization issue in view of their light weight and high force to weight ratio. The main disadvantage of SMAs is their low energy efficiency, which ranges from 5 to 7% [10]. SMA shaped as a wire, can only be contracted and extended by 7% of their total length. This imposes a limitation for the length of the joint in order to achieve a wide range of motion. Several reports have proposed control the output torque by use of SMA wires in antagonistic configuration using different design solutions [11]. Force sensors connected in series to the SMA have been used to control the output torque [12], as this can limit the overall size and weight of a miniaturised actuator.

Another challenge in robotic surgery is a soft interaction with the environment, which can be satisfied by appropriately compliant actuators, where the required position can be changed by applying an external force. In a variable impedance actuator (VIA), the compliance can be adjusted. Compliance is crucial for safety, to ensure that the robot does not harm adjacent tissues and organs. At the same time, the manipulator must be stiff enough to perform the component tasks of surgical operations. VIAs provide a solution for these conflicting requirements [13].

To achieve both a compliant behaviour and a compact design, we propose a miniaturised variable

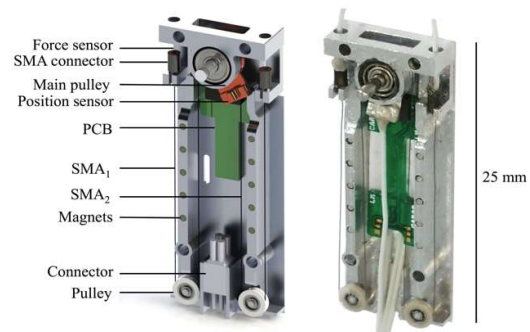


Fig. 1: Actuator design using SMA wires in antagonistic configuration. Force and position sensors are used to control the stiffness of the actuator and an electronic on-board electronics to measure the main pulley's angle. The overall size is 25 x 9 x 3.5 mm

impedance rotary actuator (VIMRA) based on SMA wire in antagonistic configuration by using miniaturised pulleys to reduce the overall length (Figure 1). The adopted antagonistic configuration, SMA wire vs. SMA wire, reduced the energy consumption needed to achieve a high maximal output torque. The two SMA wires are controlled independently, thereby achieving a compliant behaviour with changing the actuator stiffness by regulating the force provided by the opposing SMA wires.

Methods

The proposed design (Figure 1) consists of three parts: a) a frame, b) a sensory system which includes an analogue position sensor and two force sensors, c) an electronic system to control both the position and the stiffness of the joint. To reduce the friction of the system, each pulley has a miniaturized ball bearing. The frame itself was designed to work as a force sensor by incorporating strain gauges that recorded the deformation of two beams, where the SMA wires

are connected, for measuring the force applied by each. Several SMA wires of various diameter varying from 76 to 150 μm with different output torque and fast mechanical bandwidth were selected. The control system is composed of three PID controls, one for each SMA wire to control the force applied by each, and the third for control of the angular position.

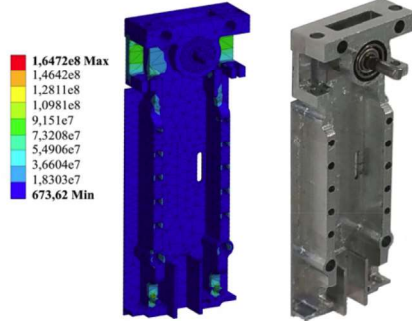


Fig. 2: Left: Finite Element Modelling for the Von Mises equivalent stress in the supporting frame. Right: A the manufactured frame.

Hardware design

VIMRA has a miniaturised compact design, and is composed of two SMA wires in antagonistic configuration, which are controlled independently. Two force sensors measure the force provided by each SMA wire, registering the output torque of the joint, which in essence is deduced from the difference between the two SMA's forces, as described by the following equation:

$$\tau = (F_1 - F_2) R_p = \Delta F R_p \quad (1)$$

where R_p is the main pulley's radius, which is 1.95 mm, and F_1 and F_2 are the forces produced by the two SMA wires on the main pulley measured by the two force sensors.

The VIMRA's frame incorporates two force sensors, and ball bearings in the main pulley, to reduce the friction. An empty space in the central part is occupied by the embedded electronic boards measuring the position of the joint. To minimize space, the position sensor is embedded in the pulley. The SMA wires are coiled round pulleys to reduce the overall length of the VIMRA. Each pulley is connected to the frame using miniaturised ball bearings to reduce friction and thus improve overall efficiency. The total weight is circa 0.7 g without the cover.

Frame design

This was optimised to reduce size and weight of the actuator by finite element modelling (FEM). The frame is made of aluminium and weighs 0.52 grams with outer dimensions of 25.0 x 9.0 x 3.5 mm.

ACTUATOR 2016, MESSE BREMEN

FEM was also used to evaluate the frame deformation and results of the stress analysis are shown in Fig. 2. The force applied by each SMA wire is 3.3 N (SMA wire with a diameter of 150 μm , can produce a force of 3.21N), in order to test the worst scenario, with a total force of 6.6 N being applied to each pulley. The stress force is concentrated in the shaft of the two ball bearings, which has a diameter of only 0.5 mm, yet the stress is still well below the

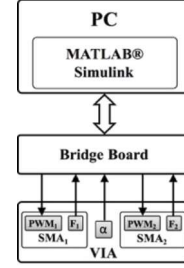


Fig. 3: Hardware control architecture

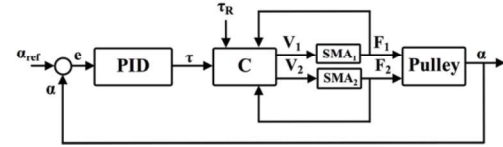


Fig. 4: Control architecture

yield stress. The other stressed part is on the top of the VIMRA, where the SMA wires are connected and powered. This is because this area was designed to provide force measurement by strain gauge sensors. The choice of the wire diameter is a trade-off between force and bandwidth, since thinner wires are faster than thicker ones, due to a heat dissipation effect. SMA wires tested in this test bed were made of nickel

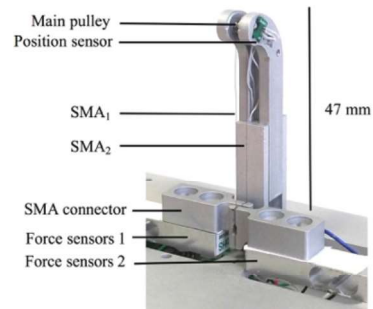


Fig. 5: Test bed designed to investigate different control solutions.

titanium with an efficiency up to 7% and can be contracted up to 5% of their total length. The performance data are reported in Tab I.

Control design

The VIMRA has an external control and its hardware

architecture is shown in Fig. 3.

Diameter (μm)	Max force (N)	Max torque (Nmm)	Max microstrains at force sensor
76	0.80	1.56	270
100	1.43	2.78	482
130	2.23	4.34	752
150	3.21	6.26	1083

Tab. I: Output performances for different SMA wires.

The hardware involved in the control is a bridge board (BB), which acquires the joint position and two force sensors, and send two independent PWM (pulse width modulation) to the SMA wires. The BB is composed of off-shelf components, with a PWM (8 bit resolution), position sensor (10 bit resolution). It exchanges data with a standalone PC, using a standard serial port (RS232), where the VIMRA's control is implemented by using Matlab® Simulink. The control implemented in the PC is shown in Fig. 4, where α_{ref} is the reference position profile, τ_R is the absolute value of the maximal output torque, V_1 and V_2 are the SMA wires' voltage, F_1 and F_2 are the force produced by each SMA wire. Two blocks are included in the control, the PID position controls, providing the output torque, and the torque control (C), providing the voltage to each SMA wire. τ_R and F_1 and F_2 are the input to the C control. The BB imposes the PWM signals to the VIMRA and receives the pulley's angle position. The voltage and current, applied to each SMA, is monitored to measure the VIMRA's power consumption, $P_i = V_i \cdot I_i$, where V_i is the voltage provided to each wire, I_i the current measured by each current sensor, and $i=1, 2$ are the SMA₁ and SMA₂.

The frame of VIMRA has an empty space in the central part to locate an embedded dedicated hardware, with a total volume of approximately 160 mm³.

Sensors design

The force sensors are serially connected to the SMA, using the rectangular beams in the VIMRA frame, in order to reduce its overall size and weight. The force provided by each SMA wire bends the beams producing stress, which is measured by miniaturised semiconductor strain gauges. These exhibit high sensitivity, although they have a large temperature drift in resistance and sensitivity; but this can be partially compensated by using a Wheatstone bridge. Each force sensor was designed to achieve 1120 micro strains when a force of 3.3 N is applied by each SMA wire. Tab. I displays the SMA wires considered for the actuator. The micro strains in the table corresponds to the strain for the maximum force of the specified SMA wire, at the location of the strain gauges. The strain gauges have not been tested in the VIMRA control loop, thus in order to investigate on

the output torque, an additional test bed was used as shown in Fig. 5.

The mechanical design of the test bed is similar to that of VIMRA and works on the same principle, the difference between the two relates to its off-shelf force sensors with bigger size. However, no additional small pulleys are used, hence the SMA wires are in a straight configuration. As miniaturised ball bearings are adopted in the small pulley of VIMRA to reduce the friction, the output torque should be similar to the one measured in the test bed.

Experiments and discussions

The VIMRA can incorporate SMA wires of different thickness as outlined in Tab. I, although in the present experiments only one diameter, 76 μm , was used, and external disturbances were applied to the main pulley to demonstrate the torque response. Fig. 6 depicts an angular position profile control $\alpha_r = A \sin(2\pi f_0 t)$, where $f_0 = 1\text{Hz}$, and $A = 25^\circ$. The figure reports the angle (α), currents (I_1 and I_2) and powers (P_1 and P_2) profile, provided by each SMA wire, respectively less than 120 mA, and 0.2 W.

Fig. 7 depicts the output torque profile, measured by using the test bed (Fig. 5) and providing a position angular profile, where $f_0 = 1\text{Hz}$, and $A = 25^\circ$. The peaks shown in the graph and highlighted in a dotted circle, represent external disturbance applied to the main pulley. In this scenario, the profile of the force shows a difference between the force sensors, and as a consequence, increased torque output.

Both forces measured by each force sensors were the same for all the position profile, as no external load was applied for most of the position profile.

The force profile shown in Fig. 7 represents the SMA wire vs. SMA wire performances in antagonistic configuration. In this configuration, when a sinusoidal angular profile is provided without external load, the active wire needs to exert force to stretch the opposite and non-active wire, because of the heat inertia and mechanical properties of the SMA wire. The force provided by the heat inertia rises with increases in the angular profile frequency, f_0 , and this is the reason why this design has selected SMA wires with thin diameter, where the heat inertia is lower than that of wires of thicker diameter. As an advantage, when a step position profile is provided, this force rises during the transitory phase but becomes negligible when the desired position is achieved. Hence, the energy consumption to keep a desired position become negligible if no external load is applied. This is an advantage of VIMRA compared with other approaches, e.g. by using one SMA wires vs. spring. This behaviour allows the VIMRA to be adopted as a robotics actuator, and represents its strength when the main tasks do not require any sinusoidal angular profile, achieving high energy efficiency and output torque.

Conclusions

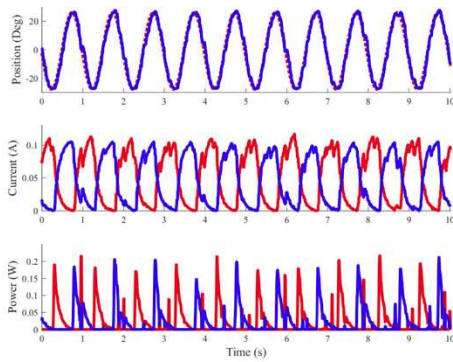


Fig. 6: Angular position close loop control, where is reported the angular position, current and power consumption..

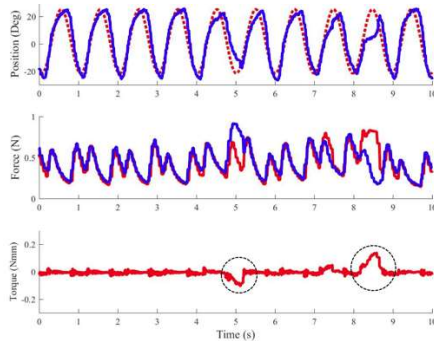


Fig. 7: Angular position control with an external disturbance. Each force sensor is connected to the base of each SMA wire to measure the applied force.

This paper presents VIMRA, a variable impedance miniaturised rotary actuator designed by using SMA wires in antagonistic configuration, implementing a control system using position sensors. Miniaturised pulleys are used to reduce the overall length of the actuator and miniaturised ball bearings to increase the overall efficiency by reducing friction. The mechanical design and the control architecture were tested using a sinusoidal angular profile.

The compact size, light weight, compliant behaviour, and particularly, the low energy consumption, enable use of this actuator in surgical robots. The hardware is robust and the sensory systems provide the scope for future studies on position and impedance control. Additional improvements are needed. These relate to control and electronic hardware design, including on-board control and force strain gauges.

Acknowledgment

The research leading to these results has received funding from the European Research Council under CARPE project supported by the EU-FP7, Grant Agreement n.665696.

References

- [1] B. Vanderborght, A. Albu-Schaeffer, A. Bicchi, E. Burdet, D. Caldwell, R. Carloni, M. Catalano, O. Eiberger, W. Friedl, G. Ganesh, M. Garabini, M. Grebenstein, G. Grioli, S. Haddadin, H. Hoppner, A. Jafari, M. Laffranchi, D. Lefeber, F. Petit, S. Stramigioli, N. Tsagarakis, M. V. Damme, R. V. Ham, L. Visser, and S. Wolf, "Variable impedance actuators: A review", *Robotics and Autonomous Systems*, vol. 61, no. 12, (2013) 1601-1614.
- [2] M. Piccigallo, U. Scarfogliero, C. Quaglia, G. Petroni, P. Valdastri, A. Menciassi, and P. Dario, "Design of a novel bimanual robotic system for single-port laparoscopy", *Mechatronics, IEEE/ASME Transactions on*, vol. 15, no. 6, 10 (2010), 871-878.
- [3] J. Peirs, D. Reynaerts, H. V. Brussel, G. D. Gersem, and H.-W. Tang, "Design of an advanced tool guiding system for robotic surgery", in *Proceedings of the 2003 IEEE International Conference on Robotics and Automation, ICRA 2003*, September 14-19, 2003, Taipei, Taiwan, vol. 2. IEEE, 9 (2003), 2651-2656.
- [7] T. L. Lam and Y. Xu, "A flexible tree climbing robot: Treebot design and implementation", in *Robotics and Automation (ICRA), 2011 IEEE International Conference on*, 5 (2011), 5849-5854.
- [8] H. Hu, P. Wang, B. Zhao, M. Li, and L. Sun, "Design of a novel snake-like robotic colonoscope", in *Robotics and Biomimetics (ROBIO), IEEE International Conference on*, 10 (2009), 1957-1961.
- [9] J. Ma, Y. Li, and S. Ge, "Adaptive control for a cable driven robot arm", in *Mechatronics and Automation (ICMA), International Conference on*, 8 (2012), 1074-1079.
- [10] C. Churchill, J. Shaw, and M. Iadicola, "Tips and tricks for characterizing shape memory alloy wire: part 2 - fundamental isothermal responses", *Experimental Techniques*, vol. 33, no. 1, 1 (2009), 51-62.
- [11] S. Huang, M. Leary, T. Ataalla, K. Probst, and A. Subic, "Optimisation of NiTi shape memory alloy response time by transient heat transfer analysis", *Materials & Design*, vol. 35, no. 0, 3 (2012), 655-663.
- [12] C. M. Lai, C. Y. Chu, and C. C. Lan, "A two degrees-of-freedom miniature manipulator actuated by antagonistic shape memory alloys", *Smart Materials and Structures*, vol. 22, no. 8, 6 (2013). 833-849.
- [13] Y. J. Kim, S. Cheng, S. Kim, and K. Iagnemma, "A novel layer jamming mechanism with tunable stiffness capability for minimally invasive surgery," *IEEE TRANSACTIONS ON ROBOTICS*, vol. 29, no. 4, 8 (2013) 1031-1041.